Supplementary Information

Solution-phase Synthesis of Cesium Lead Halide Perovskite Nanowires

Dandan Zhang[†,§,⊥] , Samuel W. Eaton[†,⊥], Yi Yu[†], Letian Dou[†,§], Peidong Yang*[,†,‡,§,∥]

[†]Department of Chemistry, [‡]Department of Materials Science and Engineering, University of California, Berkeley, CA 94720, United States

[§]Materials Sciences Division, Lawrence Berkeley National Laboratory, Berkeley, CA 94720, United States

[∥] Kavli Energy NanoSciences Institute, Berkeley, CA 94720, United States

Experimental details:

Chemicals: Cs_2CO_3 (99.9%, Aldrich), octadecene (ODE, 90%, Aldrich), oleic acid (OA, 90%, Aldrich), $PbCl_2$ (99.999%, Aldrich), $PbBr_2$ (99.999%, Aldrich), PbI_2 (99%, Aldrich), oleylamine (OLA, Aldrich, 70%), hexane (99.9%, Fisher Scientific). All chemicals were used as received without further purification.

Preparation of Cs-oleate solution: Cs-oleate solution were prepared via a reported approach developed by Protesescu *et al.*[1] Briefly, 0.4 g Cs_2CO_3 and 1.2 mL OA were loaded into a 3-neck flask along with 15 mL ODE, degassed and dried under vacuum at 120 °C for 1h, and then heated under N_2 to 150 °C until all Cs_2CO_3 reacted with OA.

Synthesis of $CsPbX_3$ nanowires: 5 mL ODE and 0.18 mmol PbX_2 were loaded into a 3-neck flask and degassed under vacuum for 1 h at 120 °C. Certain amount of OLA and OA were injected at 120 °C under N_2 (typically, 0.3 mL OLA, 0.4 mL OA for $CsPbBr_3$, 0.5 mL OLA, 0.8 mL OA for $CsPbI_3$). The temperature was raised to 150 °C and 1 h was allowed for complete dissolution of the PbX_2 salt. For the synthesis of $CsPbBr_3$ and $CsPbCl_3$ nanowires, the solution was kept at 150 °C, and 0.6 mL as-prepared Cs-oleate solution was quickly injected. After a certain duration, the reaction mixture was cooled by an ice-water bath. For $CsPbI_3$ nanowires, higher temperature (>180 °C) is needed for relative uniform nanowire growth. In a typical case, after complete dissolution of PbI_2 salt, the temperature was raised to 250 °C, and 0.6 mL of as-prepared Cs-oleate solution was injected. After 5 – 10 mins, the reaction mixture was cooled by an ice-water bath.

Isolation and purification of $CsPbX_3$ nanowires: The crude solution was cooled down with a water bath and aggregated NWs were separated by centrifugation at 6000 rpm for 5 mins and washed twice with hexane.

Characterization: Powder X-ray diffraction (XRD) patterns of the obtained products were measured on a Bruker AXS D8 Advance diffractometer with a Cu Kα source. The transmission electron microscopy (TEM), high-resolution TEM (HRTEM) images and selected-area electron diffraction (SAED) patterns were taken with a FEI Tecnai TEM at an accelerating voltage of 200 kV. Absorption spectra were collected using a Shimudzu UV-3010 PC UV-VIS-IR Scanning spectrophotometer equipped with a Shimadzu ISR-3100 integrating sphere. For PL measurement,

nanowire samples were excited with the filtered output of a Melles Griot HeCd laser (2074-S-A01, 325 nm Semrock MaxLine laser line filter) focused to an 11 μm spot. Samples were held under vacuum ($1 – 5 \times 10^{-6}$ Torr) in a Janis Research Co. ST-500 microscopy cryostat. PL was collected by a Nikon 50x objective (N.A. 0.55) in a Nikon ME600 optical microscope. Optical images were taken with an AxioCam MRc5 camera, while spectra were acquired with a fiber-coupled UV-Vis spectrometer (Acton Research Corporation SpectraPro -300i, 150/mm) equipped with a cryogenically cooled CCD (Roper Scientific 7346-0001). Atomic force microscopy (AFM) images of the nanosheets were taken using an Asylum MFP 3D in trapping mode. The perovskite nanosheets/nanowires in hexane were drop-casted on clean SiO_2 substrate for the PL and AFM measurements.

Growth mechanism: As shown in Table S1, the key parameters controlling nanowires formation are the reaction temperature, concentration of the reactants, and concentration and composition of the stabilizing agents. In the case of $CsPbBr_3$ nanowire synthesis, if the reaction temperature is too high, the stable phase during reaction will be a highly symmetric cubic phase, which lacks the inherent anisotropy of crystal structure, and thus can only yield nanocubes and large crystals. Notably, the reported reaction temperature is the temperature of the oil/salt bath, the actual reaction temperature of the reaction system will be lower.

In order to gain better understanding of the growth mechanism, more control experiments have been done. First, when only using oleylamine as surfactant, it turns out that the $PbBr_2$ does not fully dissolve. This demonstrates that oleic acid is essential for coordinating with Pb^{2+} and decomposing the precursor to form monomers. Another control experiment was carried out by changing the reaction solvent from ODE to oleylamine while maintain all other conditions. The reaction shows much slower kinetics and the yield of the nanowires is much higher (even though the size distribution becomes larger). ODE is a non-coordinating solvent, while oleylamine can serve as a capping ligand for Pb^{2+}. The slower kinetics of the control experiment implies that the binding of oleylamine to Pb^{2+} can reduce the reactivity of the Pb^{2+} precursor, and maintain a higher monomer concentration after the nucleation stage, which is essential for anisotropic growth. Also, the significant increase of the yield of nanowires in the control experiments implies that oleylamine may preferentially bind to certain facets of $CsPbX_3$, and favor the anisotropic structure growth along certain direction.

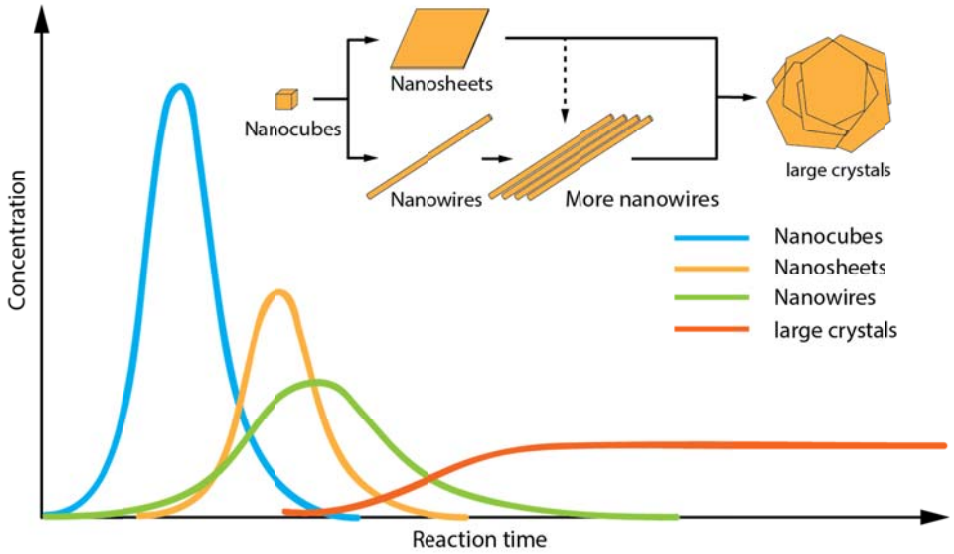

Scheme S1. A sketch showing the change of concentration of different species along with time during $CsPbBr_3$ synthesis. Inset: schematic illustration of the morphology evolution during $CsPbBr_3$ synthesis.

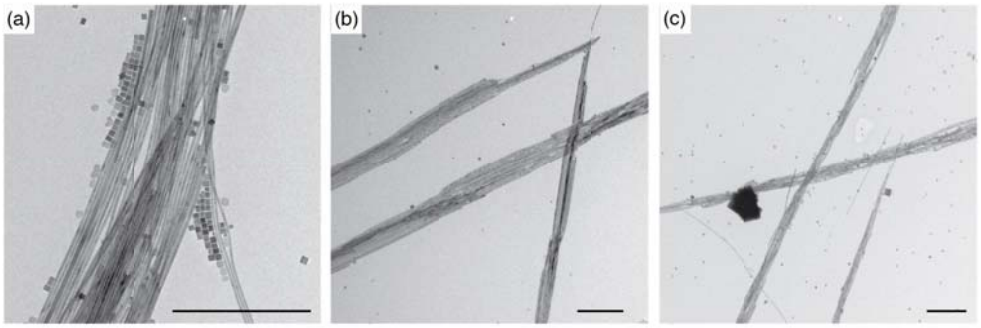

Figure S1. Representative low-resolution TEM image of as-grown $CsPbBr_3$ nanostructures. Scale bar, 500 nm.

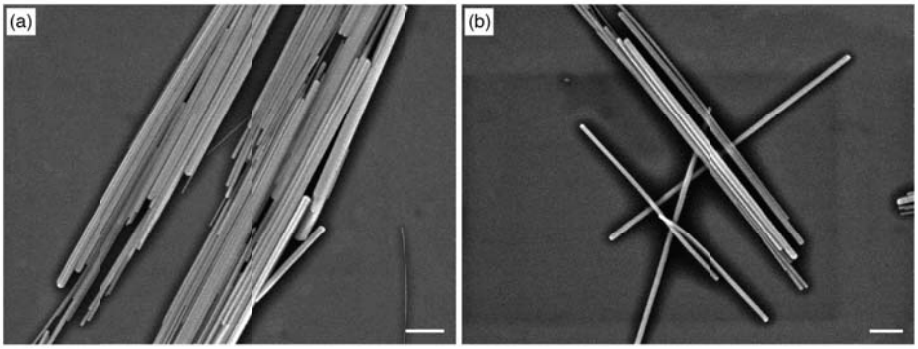

Figure S2. Representative SEM images of $CsPbI_3$ nanowires. Scale bar, 1 μm.

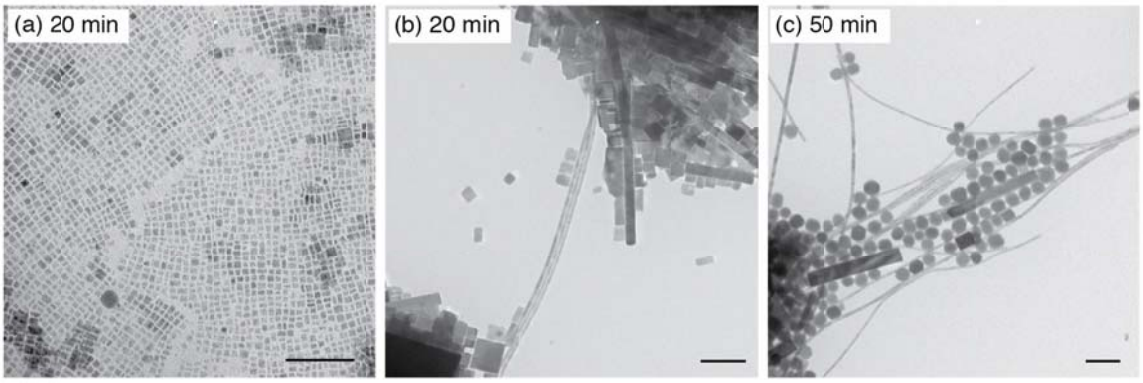

Figure S3. Shape evolution of the as-prepared $CsPbCl_3$ nanostructures with different reaction time. Scale bar, 100 nm.

Table S1. Synthetic conditions and results for $CsPbBr_3$ NWs and other morphologies.

$PbBr_2$ (g)	Cs-oleate (mL)	ODE (mL)	Oleylamine (mL)	Oleic acid (mL)	Reaction Temperature (°C)	Reaction Time (min)	Morphology	NW Yield
0.071	0.6	5	0.3	0.4	150	10	Nanocubes, nanosheets and nanowires	few
0.071	0.6	5	0.3	0.4	150	30	Nanocubes, nanosheets,nanowires with uniform diameter (~10 nm)	15-20%
0.071	0.6	5	0.3	0.4	150	90	Nanowires with uniform diameter (~10 nm), big crystals	~10%
0.072	0.6	5	0.3	0.4	150	900	500 nm crystals	0
0.069	0.6	5	0.3	0.4	250	8	20 nm cubes and some large crystals	0
0.070	0.6	5	0.5	0.5	120	60	Nanocubes and nanosheets with few nanowires	<5%
0.070	0.6	5	0.3	0	/	/	$PbBr_2$ powder does not fully dissolve	/
0.069	0.6	0	10	0.4	150	720	10 – 30 nm nanowires with some nanocrystals	60-70%
0.069	0.6	0	10	0.4	150	960	10 – 40 nm nanowires with few nanocrystals	80-90%

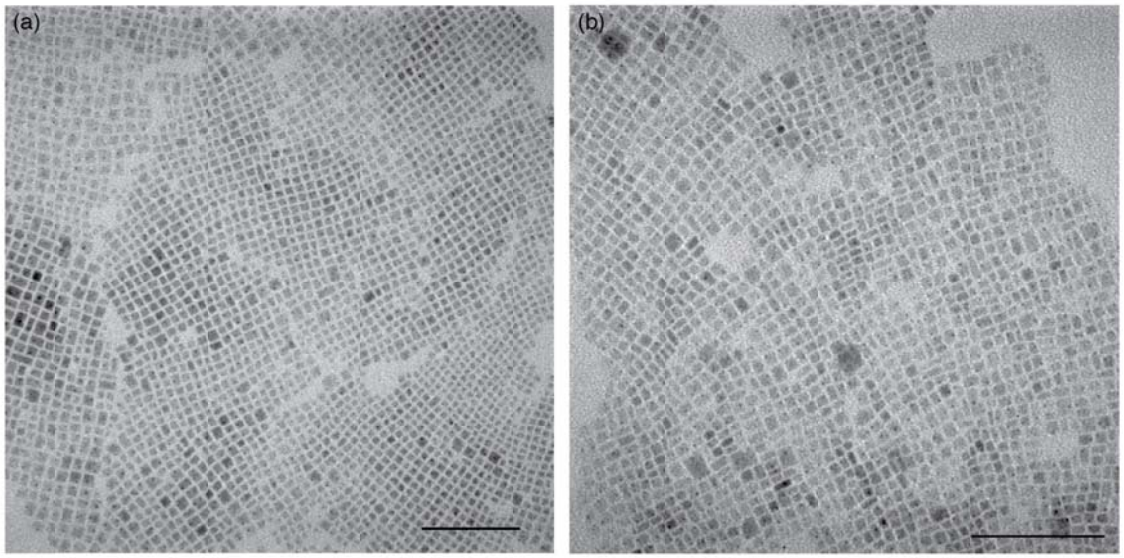

Figure S4. (a) Freshly prepared $CsPbBr_3$ nanocrystals. (b) $CsPbBr_3$ nanocrystals aged for more than two months.

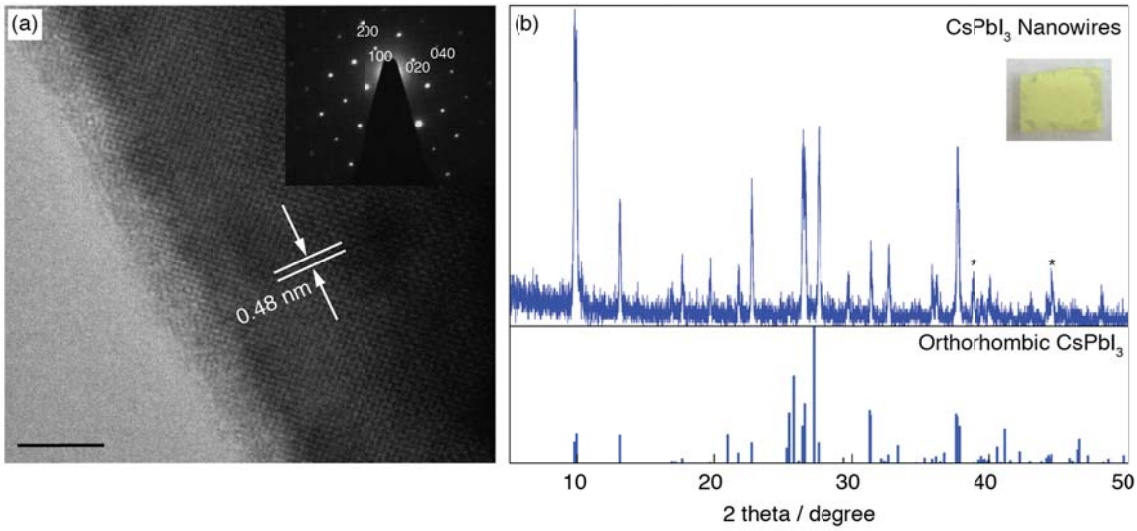

Figure S5. Structural characterization of $CsPbI_3$ nanowires. (a) Representative HR-TEM image of as-grown $CsPbI_3$ nanowire, showing the single-crystalline structure. Scale bar, 5 nm. Inset: Diffraction pattern of the same nanowire, showing <100> growth direction. (b) Experimental XRD spectrum (top) of $CsPbI_3$ nanowires, and standard XRD patterns (bottom) for orthorhombic $CsPbI_3$. Inset: $CsPbI_3$ nanowires drop-cast on glass substrate, showing yellow color. * labeled extra peaks are caused by the XRD aluminum stage.

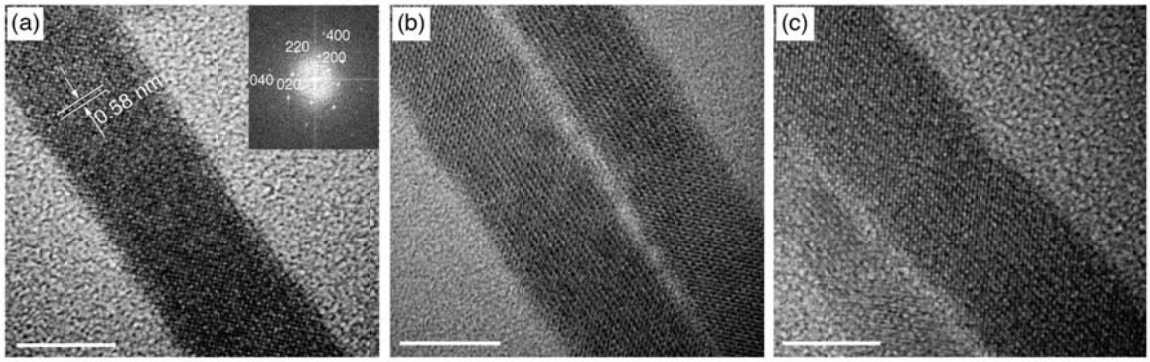

Figure S6. HR-TEM images of as-grown $CsPbBr_3$ nanowires. Scale bar, 10 nm.

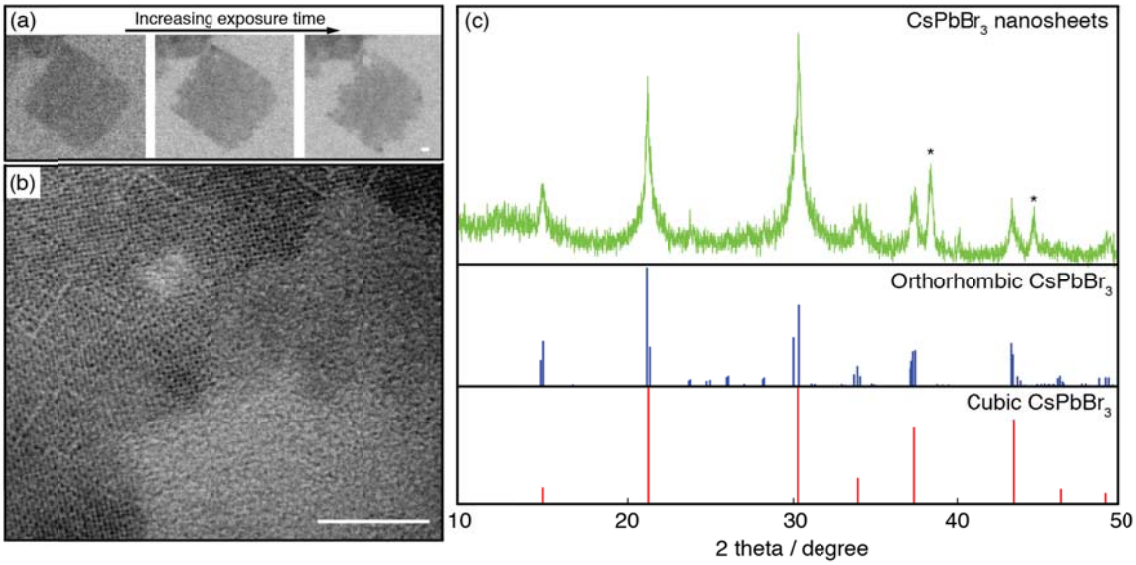

Figure **S7.** (a) Low-resolution TEM images of $CsPbBr_3$ nanosheets, showing the formation of porous structure caused by electron beam damage. (b) HR-TEM images of $CsPbBr_3$ sheets. Scale bar, 10 nm. (c) Experimental XRD spectrum (top) of $CsPbBr_3$ nanosheets, and standard XRD patterns for orthorhombic (middle) and cubic phase of $CsPbBr_3$ (bottom), * labeled extra peaks are caused by the XRD aluminum stage.

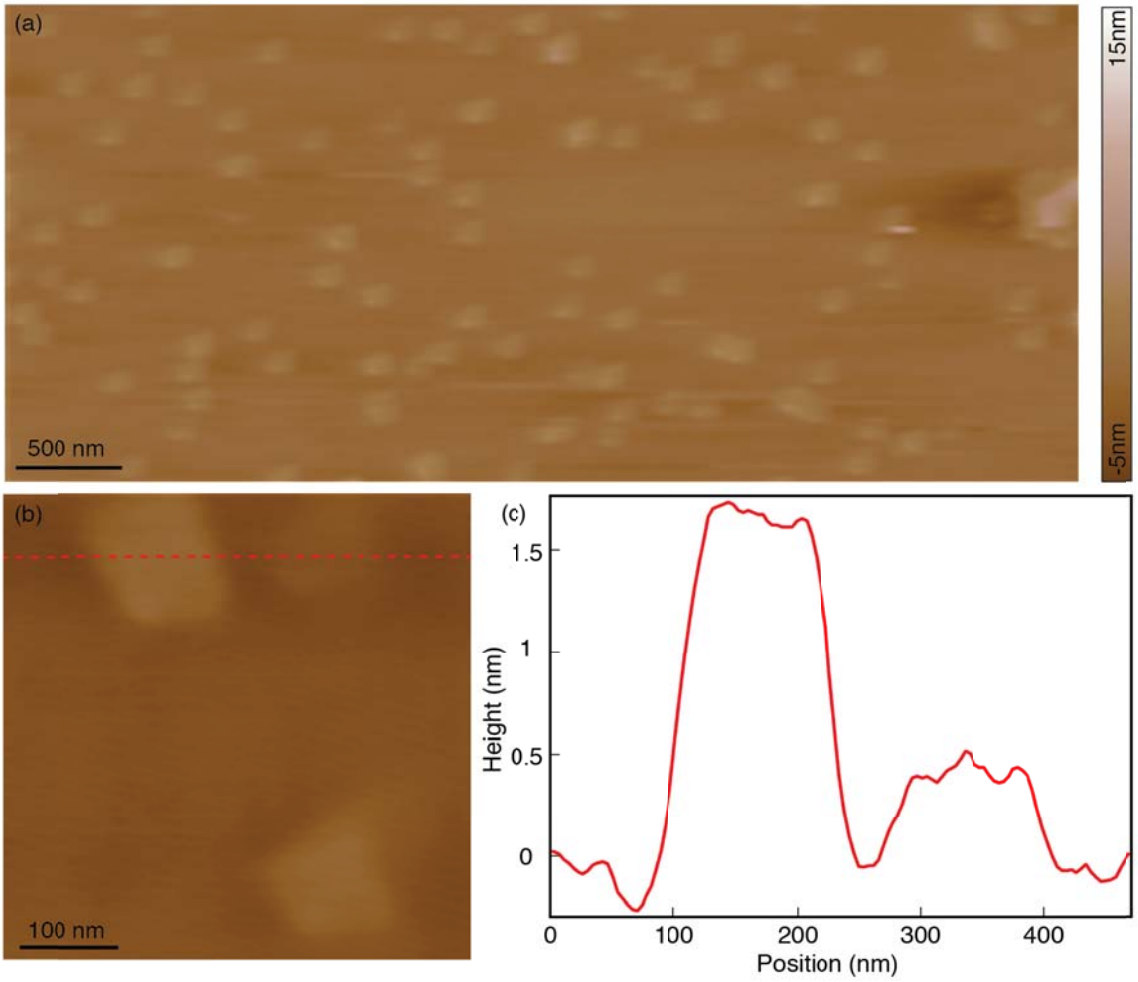

Figure S8. (a, b) AFM images and (c) height profile of $CsPbBr_3$ nanosheets, showing the thickness of the nanosheets is ranging from 0.5 – 2 nm.

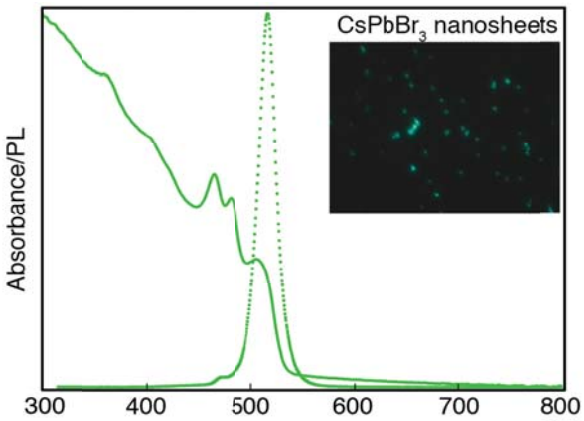

Figure S9. Typical optical absorption and PL spectra for $CsPbBr_3$ nanosheets. Inset: optical images of $CsPbBr_3$ nanosheets aggregates under laser beam.

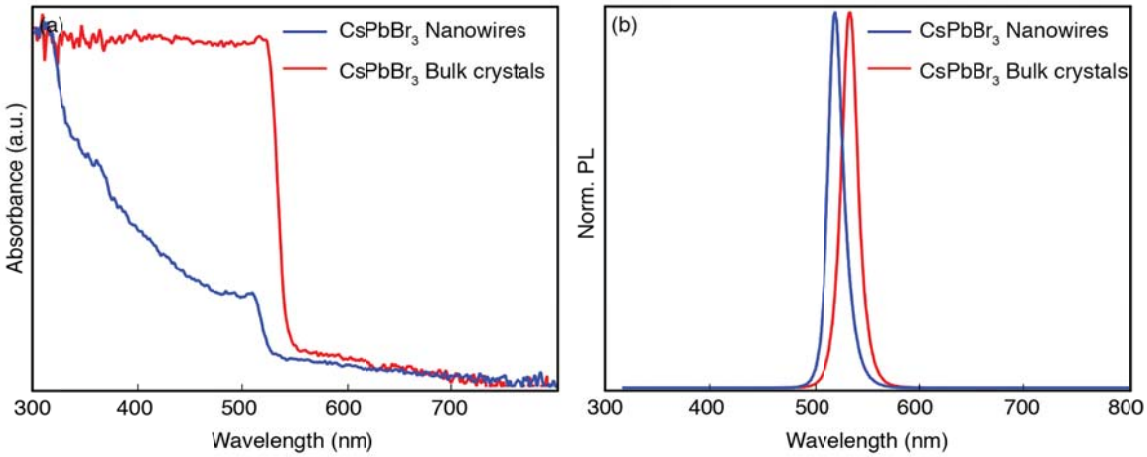

Figure S10. Typical optical absorption and PL spectra for $CsPbBr_3$ nanowires and bulk crystals.

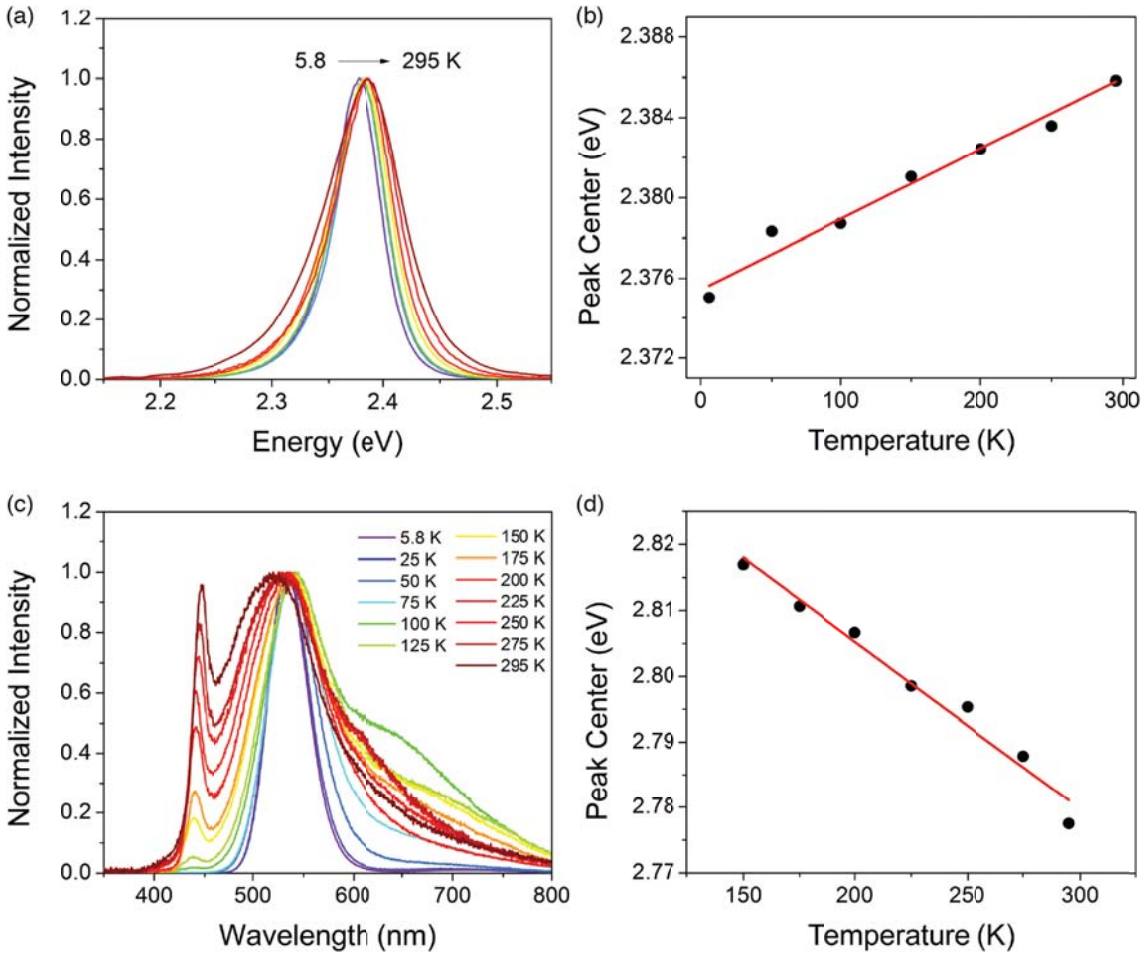

Figure S11. Temperature-dependent PL spectra and excitonic peak positions of $CsPbBr_3$ (a,b) and $CsPbI_3$ (c,d).

Photoluminescence quantum efficiency:

Table S2. Internal quantum efficiencies (IQEs) for $CsPbBr_3$ and $CsPbI_3$.

NW Composition	Internal Quantum Efficiency (IQE)
$CsPbBr_3$	0.10
$CsPbI_3$	0.18

These values were determined by integrating the total PL signal at 295 K and dividing by the total integrated signal at 5.8 K. The major assumption for this method is that all non-radiative processes are halted at low temperature, thereby providing a 100% PL quantum yield reference point. While this technique is suitable for defect emission-free materials such as $CsPbBr_3$, the existence of self-trapping in $CsPbI_3$ precludes its use as emission from self-trapped excitons cannot be assumed to be 100% efficient. Therefore, the true IQE for $CsPbI_3$ is likely much less than the calculated 0.18 above.

(1) Protesescu, L.; Yakunin, S.; Bodnarchuk, M. I.; Krieg, F.; Caputo, R.; Hendon, C. H.; Yang, R. X.; Walsh, A.; Kovalenko, M. V. *Nano Lett.* **2015**, 15, 3692.